

Extension of Petrov-Galerkin Natural Element Method to the Numerical Prediction of Stress Intensity Factors (SIF)

*Jin-Rae Cho¹⁾

¹⁾ *Department of Naval Architecture and Ocean Engineering, Hongik University,
Sejong 30016, Korea*
¹⁾ jrcho@hongik.ac.kr

ABSTRACT

This paper is concerned with an extension of Petrov-Galerkin natural element method to the numerical prediction of stress intensity factors (SIF). The interaction integral is implemented in a frame of PG-NE method in which the weighting function defined over a crack-tip integral domain is interpolated by Laplace interpolation functions. Two Cartesian coordinate systems are employed and the displacement, strains and stresses which are solved in the grid-oriented coordinate system are transformed to the other coordinate system aligned to the angled crack. The present method is validated through the numerical experiments with the angled center cracks, and the numerical accuracy is examined with respect to the grid density, crack length and angle. It is observed from the numerical results that the present method successfully and accurately evaluates the stress intensity factors of 2-D angled cracks for various crack lengths and crack angles.

1. INTRODUCTION

The numerical calculation of stress intensity factors were traditionally made by either the J -integral method or the interaction integral method. Since the late 1990s, the extension of meshfree method to this problem have been actively progressed, in particular for the calculation of stress intensity factors by the interaction integral method, inspired by the fact that the interpolation functions used in meshfree methods provide the high smoothness. Belytschko et al., (1995) and Pant et el. (2011) applied the element-free Galerkin (EFG) method to compute the singular stress fields and the stress intensity factors in 2-D fracture problems involving fatigue crack growth, dynamic crack propagation and interface cracks. Fleming et al., (1997) enriched the EFG method by adding asymptotic fields to the trial function and augmenting the basis function by the asymptotic fields, in order to accurately calculate stress intensity factors with fewer degrees of freedom. Ching and Batra (2011) enriched the polynomial basis functions in the meshless local Petrov-Galerkin (MLPG) method with the crack tip singular fields to predict the singular stress fields near a crack tip and stress intensity

factors. Rao and Rahman (2000) applied the EFG method to calculate the stress intensity factor and to simulate the crack propagation in 2-D linear fracture problems under mode-I and mixed-mode loading conditions. Fan et al. (2004) and Shi et al. (2013) enriched the partition-of-unity (POU) method to calculate the stress intensity factors of 2-D angled cracks and to solve multiple crack problems.

As an extension of our previous works (Cho and Lee, 2006b; 2006c; 2014), this paper intends to extend the Petrov-Galerkin natural element (PG-NE) method to the computation of stress intensity factors of 2-D angled cracks. To overcome the numerical integration inaccuracy caused by the discrepancy between the supports of test and basis functions, PG-NE method uses Voronoi polygon-based Laplace interpolation functions and CS-FE basis functions for the trial and test functions, respectively. The interaction integral is implemented in the frame of PG-NE method for which a crack-tip integration domain is defined by specifying the domain defining radius and the weighting function wherein is interpolated in terms of Laplace interpolation functions. The numerical experiments are carried out with the angled center cracks to examine the validity and numerical accuracy of the present method. The stress intensity factors are evaluated for various grid densities, crack lengths and crack angles and compared with the exact solution.

2. MIXED-MODE STRESS INTENSITY FACTOR

For two-dimensional planar configuration shown in Fig. 1(a), the energy release rate per unit crack extension in the x' – direction can be defined by the path-independent J – integral given by

$$J = \int_{\Gamma} \left(W \delta_{1j} - \sigma_{ij} \frac{\partial u_i}{\partial x'_1} \right) n'_j ds \quad (1)$$

using the indicial notation (i.e., $x'_1 = x'$ and $x'_2 = y'$). Here, $W = \boldsymbol{\sigma} \cdot \boldsymbol{\varepsilon} / 2$ is the strain energy density and \boldsymbol{n}' denotes the outward unit vector normal to an arbitrary path Γ enclosing the crack tip in a counter-clock wise sense. For a mixed-mode crack problem, the energy release rate J is related to the stress intensity factors such that

$$J = \frac{K_I^2 + K_{II}^2}{\bar{E}} \quad (2)$$

according to Irwin's relation (1957). Here, \bar{E} becomes E for the plane stress state and $E/(1-\nu^2)$ for the plane strain state, respectively. Note that the displacement, strains and stresses are calculated based on the grid-oriented coordinate system $\{O, x, y\}$ and then transformed to the values in the crack-line oriented coordinate system $\{O, x', y'\}$ by the chain rule.

Two stress intensity factors K_I and K_{II} in Eq. (2) can be extracted using the interaction integral which considers two equilibrium states of a cracked body. Here, state 1 is the actual equilibrium state of a body subject to the prescribed boundary conditions while state 2 denotes an auxiliary equilibrium state which corresponds to the asymptotic crack-tip displacement and stress fields. The interaction integral denoted by

$M^{(1,2)}$ for the two equilibrium states is defined by

$$M^{(1,2)} = \int_{\Gamma} \left[W^{(1,2)} \delta_{1j} - \sigma_{ij}^{(1)} \frac{\partial u_i^{(2)}}{\partial x'_1} - \sigma_{ij}^{(2)} \frac{\partial u_i^{(1)}}{\partial x'_1} \right] n'_j ds \quad (3)$$

where $W^{(1,2)}$ denotes the mutual strain energy density defined by $W^{(1,2)} = [\boldsymbol{\sigma}^{(1)} \cdot \boldsymbol{\varepsilon}^{(2)} + \boldsymbol{\sigma}^{(2)} \cdot \boldsymbol{\varepsilon}^{(1)}] / 2$.

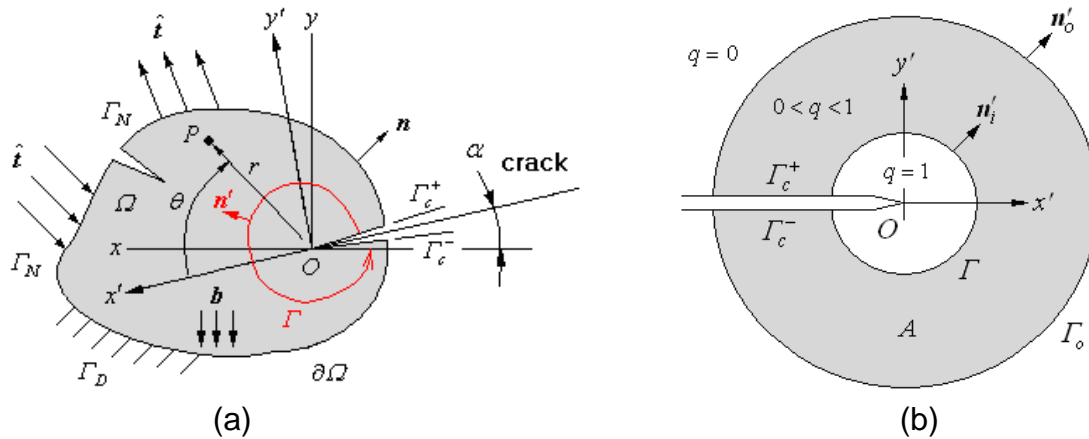


Fig.1 (a) A cracked 2-D linear elastic body, (b) an integral domain A and the weighting function $q(x)$

The line integral (3) is not always best for numerical calculation because the integration of displacement gradients, strains and stresses of states 1 and 2 along the non-regular arbitrary path Γ becomes rather painstaking. Thus, it is desired to be transformed into an area integral form, for which Eq. (3) is firstly rewritten as

$$M^{(1,2)} = \int_C \left[\sigma_{ij}^{(1)} \frac{\partial u_i^{(2)}}{\partial x'_1} + \sigma_{ij}^{(2)} \frac{\partial u_i^{(1)}}{\partial x'_1} - W^{(1,2)} \delta_{1j} \right] qm'_j ds \quad (4)$$

by extending the path Γ to $C = \Gamma + \Gamma_c^- + \Gamma_c^+ + \Gamma_o$ along two crack faces as shown in Fig. 2 and by multiplying a sufficiently smooth weighting function $q(x)$. It is not hard to realize that Eqs. (3) and (4) become identical when $q(x)$ becomes unity on Γ and vanishes on Γ_o , together with the fact that the crack faces are traction free and straight in the darkened donut-type region A . By taking the divergence theorem to Eq. (4) and letting the inner path Γ be shrunk to the crack tip, the transformed line integral (4) ends up with

$$M^{(1,2)} = \int_A \left[\sigma_{ij}^{(1)} \frac{\partial u_i^{(2)}}{\partial x'_1} + \sigma_{ij}^{(2)} \frac{\partial u_i^{(1)}}{\partial x'_1} - W^{(1,2)} \delta_{1j} \right] \frac{\partial q}{\partial x'_j} dA \quad (5)$$

All the quantities in Eq. (5) are evaluated with respect to the crack-line oriented Catesian coordinate system $\{O, x', y'\}$.

3. INTERACTION INTEGRAL BY PG-NE METHOD

The boundary value problem of 2-D linear elasticity in the strong form is converted to the weak form according to the usual virtual work principle: Find $\mathbf{u}(\mathbf{x})$ such that

$$\int_{\Omega} \boldsymbol{\varepsilon}(\mathbf{v}) : \boldsymbol{\sigma}(\mathbf{u}) d\mathbf{v} = \int_{\Omega} \mathbf{b} \cdot \mathbf{v} d\mathbf{v} + \int_{\Gamma_N} \hat{\mathbf{t}} \cdot \mathbf{v} ds \quad (6)$$

for every admissible displacement field $\mathbf{v}(\mathbf{x})$ in the grid-oriented Cartesian coordinate system $\{O, x, y\}$. In order for the Petrov-Galerkin natural element approximation using a given non-convex natural element grid \mathfrak{S}_{NEM} composed of N grid points and Delaunay triangles as shown in Fig. 2(a), trial and test displacement fields $\mathbf{u}(\mathbf{x})$ and $\mathbf{v}(\mathbf{x})$ are expanded as

$$\mathbf{u}_h(\mathbf{x}) = \sum_{J=1}^N \mathbf{u}_J \phi_J(\mathbf{x}) = \boldsymbol{\Phi} \bar{\mathbf{u}}, \quad \mathbf{v}_h(\mathbf{x}) = \sum_{I=1}^N \mathbf{v}_I \psi_I(\mathbf{x}) = \boldsymbol{\Psi} \bar{\mathbf{v}} \quad (7)$$

with Laplace interpolation functions $\phi_J(\mathbf{x})$ shown in Fig. 2(b) and CS-FE basis functions $\psi_I(\mathbf{x})$. The reader may refer to the references (Cho and Lee, 2006a; Cho et al., 2013) for more details on the CS-FE basis function defined on three-node triangular elements and the definition of Laplace interpolation functions. Meanwhile, $\boldsymbol{\Phi}$ and $\boldsymbol{\Psi}$ denote $(2 \times 2N)$ matrices containing N basis functions ϕ_J and ψ_I , and $\bar{\mathbf{u}}$ and $\bar{\mathbf{v}}$ are the $(2N \times 1)$ nodal vectors, respectively.

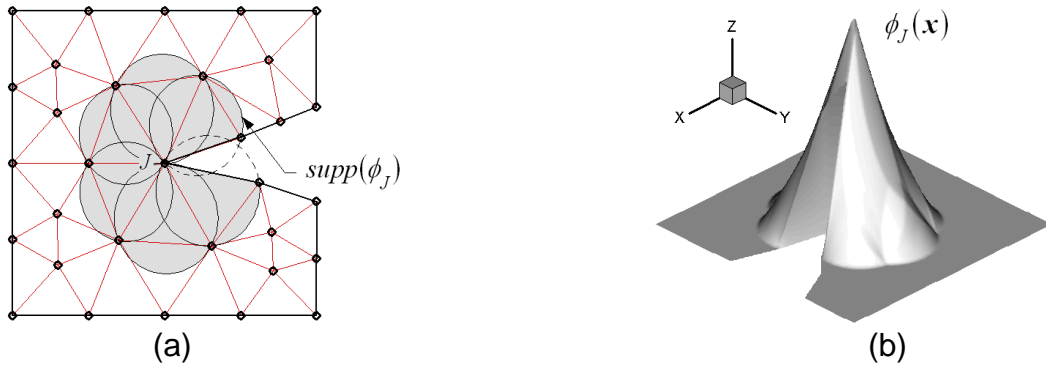


Fig. 2. (a) Non-convex NEM grid \mathfrak{S}_{NEM} , (b) Laplace interpolation function $\phi_J(\mathbf{x})$

Substituting Eq. (7) into Eq. (6) leads to the simultaneous linear equations in matrix form given by

$$[\mathbf{K}] \bar{\mathbf{u}} = \{\mathbf{F}\} \quad (8)$$

Here, the global stiffness matrix $[\mathbf{K}]$ and the global load vector $\{\mathbf{F}\}$ are constructed as following

$$[\mathbf{K}] = \sum_{I=1}^N \mathbf{K}_I, \quad \{\mathbf{F}\} = \sum_{I=1}^N \mathbf{F}_I \quad (9)$$

with the node-wise stiffness matrices and load vectors defined by

$$\mathbf{K}_I = \int_{\Omega_v^I} (\mathbf{L}\Psi)^T \mathbf{E}(\mathbf{L}\Phi) dv \quad (10)$$

$$\mathbf{F}_I = \int_{\Omega_v^I} \Psi^T \mathbf{b} dv + \int_{\Gamma_N \cap \Omega_v^I} \Psi^T \hat{\mathbf{t}} ds \quad (11)$$

Here, $\Omega_v^I = \text{supp}(\psi_I(x))$ indicates the support of I -th CS-FE basis function and \mathbf{E} indicates the (3×3) material constant matrix of linear elasticity. It is noted that the numerical integration in the natural element method is carried out Delaunay triangle by Delaunay triangle.

The weighting function $q(x)$ specified in Fig. 1(b) should be sufficiently smooth such that its differentiation in the interaction integral (5) is integrable. In the current study, Laplace interpolation function $\phi_j(x)$ depicted in Fig. 2(b) which is also used for the trial function is used. Meanwhile, the crack-tip integral domain A is chosen by specifying its radius r_{int} as represented in Fig. 3. The value of unity is assigned to all the nodes within the circle, while the value of zero is specified to the remaining nodes within a whole NEM grid. Then, from the linearity property of Laplace interpolation function (Cho et al., 2013), a darkened rectangular region has the value of unity and its boundary serves as an interior path Γ shown in the previous Fig. 1(b). Meanwhile, another union of grayed Delaunay triangles have the value $0 \leq q \leq 1$ and its boundary becomes the outer path Γ_o . In other words, the union of grayed Delaunay triangles automatically becomes the integral domain A .

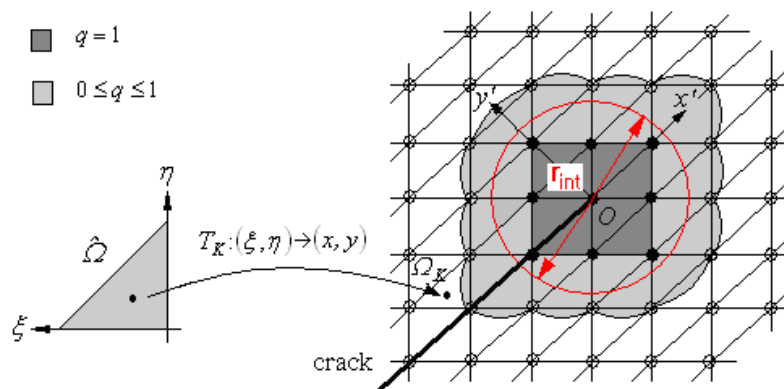


Fig. 3. The construction of the integral domain A and the weighting function $q(x)$

Let us denote M_A be the total number of grayed Delaunay triangles within the integral domain A , then the interaction integral (5) is integrated triangle by triangle such that

$$M^{(1,2)} = \sum_{K=1}^{M_A} M_K^{(1,2)} \quad (12)$$

with $M_K^{(1,2)}$ being the triangle-wise interaction integrals. It is because the gradient of weighting function $\partial q / \partial x'_j$ vanishes outside the integral domain A . Here, each triangle-wise interaction integral is computed by

$$M^{(1,2)} = \sum_{\lambda=1}^{INT} \left[\sigma_{ij}^{(1)} \frac{\partial u_i^{(2)}}{\partial x'_j} + \sigma_{ij}^{(2)} \frac{\partial u_i^{(1)}}{\partial x'_j} - W^{(1,2)} \delta_{1j} \right]_{x_\lambda} \frac{\partial q}{\partial x'_j} \Big|_{x_\lambda} w_\lambda |J|_{x_\lambda} \quad (13)$$

using the chain rule and Gauss quadrature rule, in which INT , x_λ and w_λ indicate the total number of integration points, sampling points and weights, respectively. Note that the sampling points x_λ in Ω_K and the Jacobian $|J|_{x_\lambda}$ are calculated using the geometry transformation T_K defined by

$$T_K : x_\lambda = \sum_{i=1}^3 x_i \psi_i(\xi, \eta)_\lambda, \quad y_\lambda = \sum_{i=1}^3 y_i \psi_i(\xi, \eta)_\lambda \quad (14)$$

between Ω_K in NEM grid and the master triangle element $\hat{\Omega}$. Here, $\{x_i, y_i\}$ are the coordinates of three nodes in each Delaunay triangle, $(\xi, \eta)_\lambda$ the Gauss points in $\hat{\Omega}$, and ψ_i the triangular shape functions.

4. NUMERICAL EXPERIMENT

Fig. 4(a) shows a square plate of $L=20in$ with an angled center crack which is in plane stress condition and subjected to a far-field uniform vertical distributed load σ equal to unity. The material properties are as follows: $E=3.0 \times 10^7 psi$ and $\nu=0.25$, and the crack of length $2a$ is oriented with an angle α with respect to the negative x -axis. Uniform NEM grid shown in Fig. 4(b) is used and the total number of grid points is taken variable for the parametric experiment. According to Yau et al. (1980) and Dolbow and Gosz (2002), the stress intensity factors which are analytically expressed in terms of the angle α are given by

$$K_I = \sigma \sqrt{\pi a} \cos^2 \alpha, \quad K_{II} = \sigma \sqrt{\pi a} \sin \alpha \cos \alpha \quad (15)$$

with a being the half crack length. For the convergence experiment with respect to the density of uniform NEM grid, the crack angle α is set by 45° and the grid density-dependent half crack length a varies from $3.394in$ to $5.657in$ as given in Table 2.

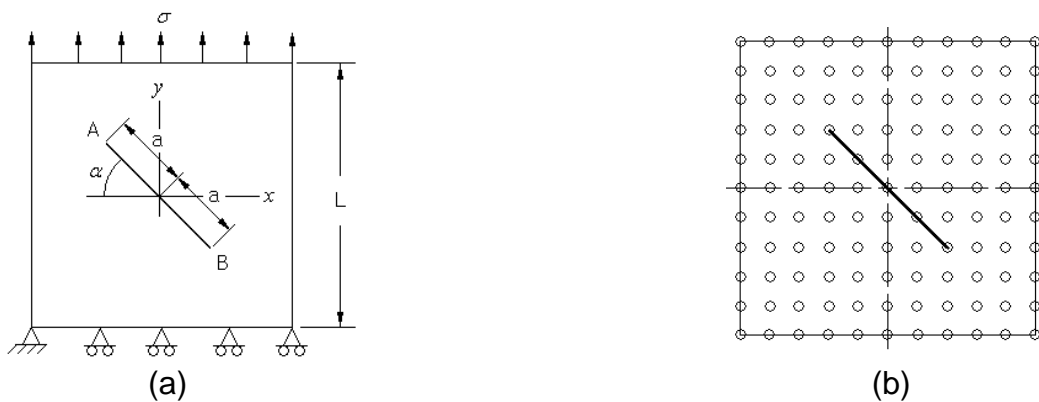


Fig. 4. (a) A square plate with an angled center crack under a uniform tensile distributed load, (b) uniform NEM grid.

Referring to Table 1, five uniform NEM grids are used and the ratios K_I / K_I^{anal} and K_{II} / K_{II}^{anal} of stress intensity factor are calculated at two crack tips A and B . As in the previous example, 13 Gauss points are used for both the NEM structural analysis and the interaction integral. It is clearly observed from Table 1 and Fig. 5 that the ratios of stress intensity factor approach unity as the grid density increases such that the NEM grids higher than 30×30 provide the stress intensity factors with the maximum relative error less than 2.0%. Thus, it has been verified that PG-NE method accurately predicts the stress intensity factors of angled crack with the practically reasonable grid density.

Table 1. Variation of stress intensity factors to the grid density

NEM grid	Half crack length $a(in)$	Total number of nodes	K_I / K_I^{anal}		K_{II} / K_{II}^{anal}	
			tip A	tip B	tip A	tip B
50×50	3.394	2601	1.0147	0.9909	0.9940	1.0053
40×40	3.536	1681	1.0180	1.0035	0.9907	0.9810
30×30	3.771	961	1.0105	0.9529	1.0268	0.9792
20×20	4.243	441	0.9781	1.0602	1.0553	0.9051
10×10	5.657	121	0.8964	0.8599	0.8435	0.8656

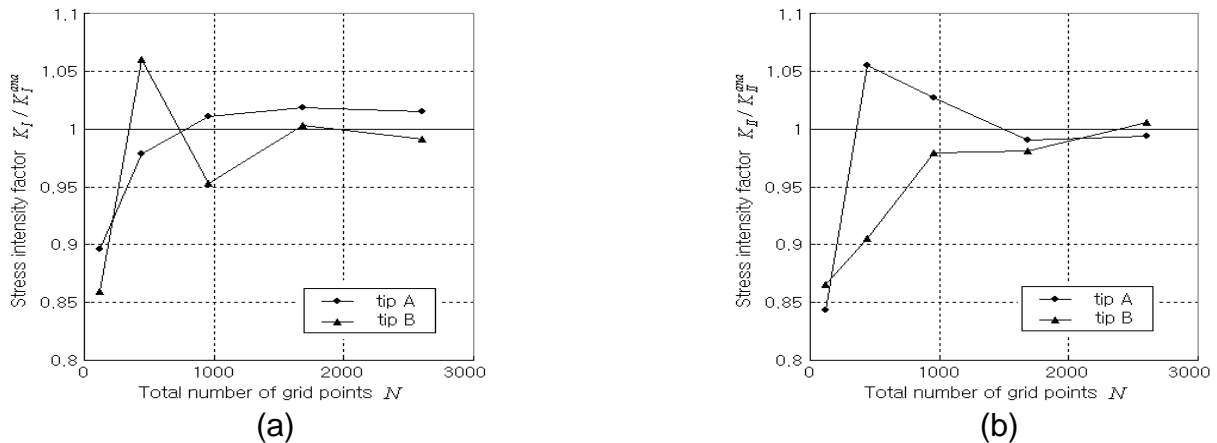


Fig. 5. Stress intensity factors to the total number of nodes: (a) K_I / K_I^{ana} , (b) K_{II} / K_{II}^{ana}

Fig. 6(a) represents the variation of stress intensity factors to the half crack length when the crack angle is 45° , where the exact values are calculated using Eq. (15). A 40×40 uniform NEM grid is used based on the previous convergence experiment and the stress intensity factors are calculated at crack tip B . It is observed that the stress intensity factors K_I and K_{II} are in good agreement with the exact values for the relative crack lengths of $0.071 \leq a/L \leq 0.354$. The maximum relative error equal to 5.66% with respect to the exact solution is occurred at $a/L = 0.247$. Thus, it has been justified that the present method provides accurate stress intensity factors of center angled crack for various crack lengths. Fig. 6(b) represents the comparison of SIF ratios between the present method and XFEM by Liu et al. (2004). Since there is difficulty in keeping exactly the relative crack length of 0.05 for different crack angles, the SIF

ratios are taken for the comparison between two methods. It is observed that the present method provides the numerical accuracy similar to XFEM.

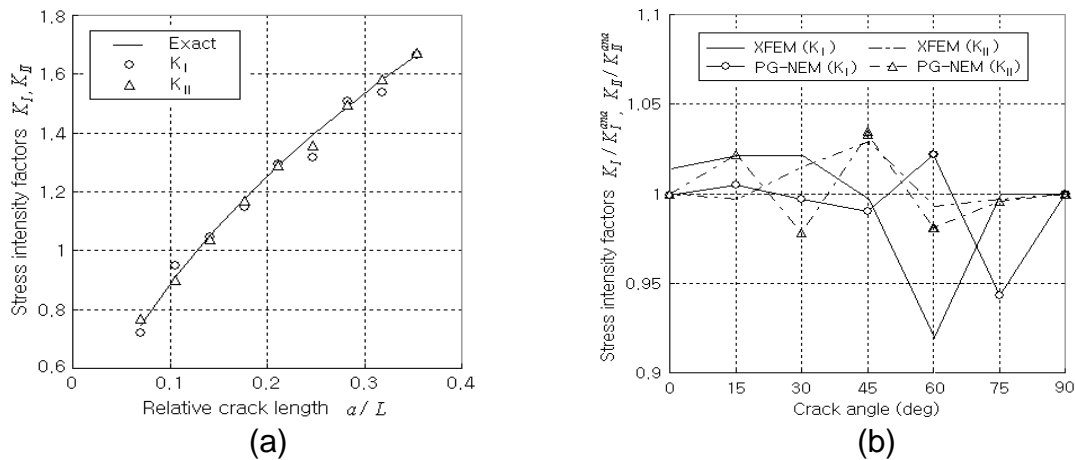


Fig. 6. (a) Stress intensity factors to the half crack length, (b) ratios of stress intensity factor to the crack angle.

CONCLUSION

Through the numerical experiment with the angled center crack to the grid density, it has been confirmed that the *SIF* ratios approach unity as the grid density increases such that the maximum relative error with respect to the exact solution is less than 20% when NEM grid is finer than 30×30 . Furthermore, it has been observed that the stress intensity factors K_I and K_{II} at both crack tips are in good agreement with the exact values for the relative crack lengths of $0.071 \leq a/L \leq 0.354$. In addition, it has been verified that the numerical accuracy similar to XFEM for a wide range of crack angles.

ACKNOWLEDGEMENT

This research was supported by Basic Science Research Program through the National Research Foundation of Korea (NRF) funded by the Ministry of Education (Grant No. NRF-2017R1D1A103028879).

REFERENCES

- Belytschko, T., Lu, Y.Y., Gu, L. and Tabbara, M. (1995), "Element-free Galerkin methods for static and dynamic fracture", *Int. J. Solids Struct.*, **32**(17-18), 2547-2570.
- Ching, H.K. and Batra, R.C. (2001), "Determination of crack tip fields in linear elastostatics by the meshless local Petrov-Galerkin (MLPG) method", *Comput. Model. Eng. Sci.*, **2**(2), 273-289.
- Cho, J.R. and Lee, H.W. (2006a), "A Petrov-Galerkin natural element method securing the numerical integration accuracy", *J. Mech. Sci. Technol.*, **20**(1), 94-109.
- Cho, J.R. and Lee, H.W. (2006b), "2-D large deformation analysis of nearly incompressible body by natural element method", *Comput. Struct.*, **84**, 293-304.

- Cho, J.R., Lee, H.W. and Yoo, W.S. (2013), "Natural element approximation of Reissner-Mindlin plate for the locking-free numerical analysis of plate-like thin elastic structures", *Comput. Methods Appl. Mech. Engrg.*, **256**, 17-28.
- Cho, J.R. and Lee, H.W. (2014), "Calculation of stress intensity factors in 2-D linear fracture mechanics by Petrov-Galerkin natural element method", *Int. J. Numer. Methods Engrg.*, **98**, 819-839.
- Dolbow, J. and Gosz, M. (2002), "On the computation of mixed-mode stress intensity factors in functionally graded materials", *Int. J. Solids Struct.*, **39**(9), 2557-2574.
- Fan, S.C., Liu, X. and Lee, C.K. (2004), "Enriched partition-of-unity finite element method for stress intensity factors at crack tips", *Comput. Struct.*, **82**, 445-461.
- Fleming, M., Chu, Y.A., Moran, B. and Belytschko, T. (1997), "Enriched element-free Galerkin methods for crack tip fields", *Int. J. Numer. Methods Engrg.*, **40**, 1483-1504.
- Irwin, G.R. (1957), "Analysis of stresses and strains near the end of a crack traveling a plate", *J. Appl. Mech.*, **24**, 361-364.
- Liu, X.Y., Xiao, Q.Z. and Karihaloo, B.L. (2004), "XFEM for direct evaluation of mixed mode SIFs in homogeneous and bi-materials", *Int. J. Numer. Methods Engrg.*, **59**, 1103-1118.
- Pant, M., Singh, I.V. and Mishra, B.K. (2011), "Evaluation of mixed mode stress intensity factors for interface cracks using EFGM", *Appl. Math. Modell.*, **35**(7), 3443-3459.
- Rao, B.N. and Rahman, S. (2000), "An efficient meshless method for fracture analysis of cracks", *Comput. Mech.*, **26**, 398-408.
- Shi, J., Ma, W. and Li, N. (2013), "Extended meshless method based on partition of unity for solving multiple crack problems", *Meccanica*, **43**(9), 2263-2270.
- Yau, J.F., Wang, S.S. and Corten, H.T. (1980), "A mixed-mode crack analysis of isotropic solids using conservation laws of elasticity", *J. Appl. Mech.*, **47**, 335-341.